Synthesis and Characterization of High-nuclearity Osmium–Platinum Cluster Compounds. The Molecular Structures of $[Os_6Pt_2(CO)_{16}(C_8H_{12})_2]$ and $[Os_6Pt_2(CO)_{16}(C_8H_{12})\{P(OMe)_3\}_2]$ (C_8H_{12} = Cyclo-octa-1,5-diene)†

Christiane Couture and David H. Farrar*
Lash Miller Chemical Laboratories, 80 St. George Street, University of Toronto, Toronto, Canada M5S 1A1

The reaction of $[Os_6(CO)_{18-n}(NCMe)_n]$ (n = 1 or 2) with $[Pt(C_8H_{12})_2]$ (C_8H_{12} = cyclo-octa-1,5-diene) results in the formation of $[Os_6Pt_2(CO)_{17}(C_8H_{12})_2]$ (**1**) and $[Os_6Pt_2(CO)_{16}(C_8H_{12})_2]$ (**2**) respectively. Complex (**1**) is known to have a Pt-bicapped octahedral geometry. Complex (**2**) crystallizes in the monoclinic space group $C2/c$ with a = 21.178(3), b = 11.683(2), c = 17.383(2) Å, β = 113.83(1)°, Z = 4. The structure has been refined to R' = 0.034 (R = 0.044) for 2 675 unique diffractometer data. The complex possesses the unusual metal-core geometry of two edge-fused Os tetrahedra, one of which is Pt-bicapped. This cluster is a 108-electron system and its metallic framework cannot be explained by any of the conventional electron-counting schemes. The cluster is formally electronically unsaturated and this is reflected in its apparent reactivity. Complex (**2**) reacts immediately with CO or $P(OMe)_3$ to yield cluster (**1**) or complex $[Os_6Pt_2(CO)_{16}(C_8H_{12})\{P(OMe)_3\}_2]$ (**3**), respectively. Complex (**3**) crystallizes in the monoclinic space group $P2_1/c$ with a = 19.160(4), b = 10.963(2), c = 21.277(6) Å, β = 99.40(2)°, Z = 4, and the molecular structure has been refined to R' = 0.073 (R = 0.086) for 2 818 unique data. The molecular geometry of (**3**) can be described as a bicapped tetrahedron of Os atoms having two Pt-capped faces. Complex (**3**) is also a 108-electron system but its geometry can be rationalized by using any of the electron-counting schemes. Cluster (**3**) reacts immediately with CO to give a compound which has the same metal-core geometry as (**1**). The relationship between the structures of (**1**), (**2**), and (**3**) is discussed briefly in terms of transformations of the mixed-metal cluster skeleton.

There are a number of examples of transition-metal cluster compounds which undergo reversible geometry changes upon ligand addition. One example is the reaction[1] of CO and $[Os_5(CO)_{16}]$, which generates $[Os_5(CO)_{19}]$, and the heating of $[Os_5(CO)_{19}]$ to give $[Os_5(CO)_{16}]$ plus CO. In many of these systems the geometry changes have been rationalized by considering a stepwise opening or closing of the metal polyhedron. While this approach is useful for conceptualizing the rearrangements, it is not necessarily related to the actual reaction pathway. One possible way to obtain more information about the pathway by which the metal-core structures interconvert is through the study of mixed-metal cluster compounds. This allows mapping of specific sites in the precursor clusters into sites in the products.

Mixed-metal clusters have been synthesized by a number of general routes including pyrolyses, addition to co-ordinatively unsaturated clusters, redox condensations, and reaction of carbonylmetalates with metal halides.[2] Our approach to preparing mixed-metal cluster compounds consists of the reaction of a cluster and a complex, both of which contain weakly bound ligands. Thus, the reaction of $[Os_6(CO)_{18-n}(NCMe)_n]$ with $[Pt(C_8H_{12})_2]$ (C_8H_{12} = cyclo-octa-1,5-diene) leads to the formation of $[Os_6Pt_2(CO)_{18-n}(C_8H_{12})_2]$, where n = 1 or 2. The two mixed-metal clusters differ only in the number of carbonyl ligands in their chemical formula, but this results in different solid-state metallic skeletons. A preliminary report of part of this work has already been published.[3] We have extended this system by examining the interconversion of the two aforementioned clusters and also have isolated an intermediate geometry.

Results and Discussion

The reaction of $[Os_6(CO)_{18-n}(NCMe)_n]$ (n = 1 or 2)[4] with two equivalents of $[Pt(C_8H_{12})_2]$ at ambient temperature gives a dark brown solid after evaporation of the solvent. The products have been separated by t.l.c. giving three or four major compounds which together with the other minor components account for 80% of the brown solid. The reactions are summarized in the Scheme and i.r. data are presented in Table 1. Only two mixed-metal clusters obtained from this reaction are presented here; the other products will be reported elsewhere.

For n = 1, the mauve band on the t.l.c. plate is $[Os_6Pt_2(CO)_{17}(C_8H_{12})_2]$ (**1**), obtained in 20% yield. The crystal structure of (**1**) has been reported[5] and its metal-core geometry may be described as a regular octahedron of osmium atoms with two face-capping $Pt(C_8H_{12})$ fragments. In terms of electron-counting, (**1**) is a 110-electron system and the observed structure is in agreement with that proposed by Wade's skeletal electron-counting scheme[6] when extended to include clusters which have m metal atoms and m or (m − 1) skeletal electron pairs. The bicapped-octahedral cluster core geometry is the same as found for the isoelectronic homometallic osmium cluster anion[7] $[Os_8(CO)_{22}]^{2-}$.

For n = 2, the brown band on the t.l.c. plate is $[Os_6Pt_2(CO)_{16}(C_8H_{12})_2]$ (**2**), isolated in 15% yield. Dark brown crystals of (**2**) suitable for X-ray analysis were obtained from the slow evaporation of an ethyl acetate solution. Figure 1 illustrates the molecular structure of (**2**) and the intramolecular

† Hexadecacarbonylbis[(η^4-cyclo-octa-1,5-diene)platinio]-*polyhedro*-hexaosmium (6 *Pt–Os*)(11 *Os–Os*) and hexadecacarbonyl[bis(trimethyl phosphite)platinio][(η^4-cyclo-octa-1,5-diene)platinio]-*polyhedro*-hexaosmium (6 *Pt–Os*)(11 *Os–Os*).

Supplementary data available (No. SUP 56517, 7 pp.): H-atom co-ordinates, thermal parameters. See Instructions for Authors, *J. Chem. Soc., Dalton Trans.*, 1986, Issue 1, pp. xvii—xx. Structure factors are available from the editorial office.

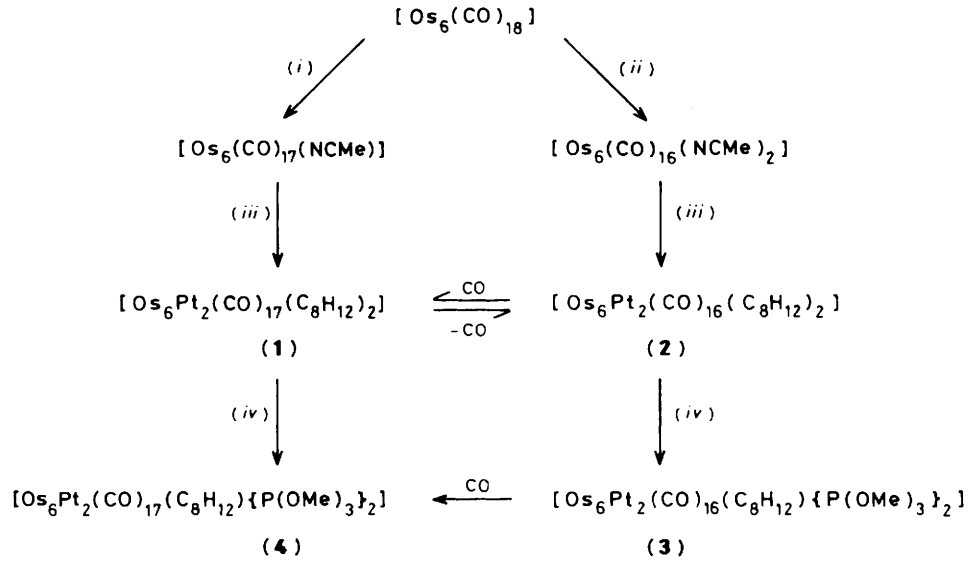

Scheme. Synthesis and some reactions of high-nuclearity Os–Pt clusters. (*i*) Slow addition of 1 mol equiv. of Me_3NO, in $MeCN–CH_2Cl_2$; (*ii*) 2 mol equiv. of Me_3NO; (*iii*) $[Pt(C_8H_{12})_2]$, in CH_2Cl_2 stirred for 16 h; (*iv*) addition of 2 mol equiv. of $P(OMe)_3$, in CH_2Cl_2

Table 1. Infrared carbonyl stretching bands (cm^{-1})

Complex	ν(CO)
(1) $[Os_6Pt_2(CO)_{17}(C_8H_{12})_2]$[a]	2 069w, 2 033s, 2 020vs, 1 978m
(3) $[Os_6Pt_2(CO)_{16}(C_8H_{12})\{P(OMe)_3\}_2]$[a]	2 067m, 2 042vs, 2 008vs, 1 990m, 1 963w, 1 949w (sh), 1 913w,br
(4) $[Os_6Pt_2(CO)_{17}(C_8H_{12})\{P(OMe)_3\}_2]$[a]	2 072m, 2 029vs, 2 011m, 1 989m, 1 975w, 1 964br
(2) $[Os_6Pt_2(CO)_{16}(C_8H_{12})_2]$[a]	2 075m, 2 057vs, 2 032m (sh), 2 017s, 2 009s, 1 988s, 1 960w
(2)[b]	2 076m, 2 058vs, 2 034m (sh), 2 021s, 2 010s, 1 994m
(2)[c]	2 075m, 2 056vs, 2 030s (sh), 2 016vs, 2 008s (sh), 1 988s, 1 958w
(2)[d]	2 076m, 2 058vs, 2 031s (sh), 2 018vs, 1 990s, 1 960m
(2)[e]	2 088w, 2 077m, 2 063vs, 2 049s, 2 035s, 2 027vs (sh), 2 017vs, 1 996s, 1 985s, 1 968m, 1 955m, 1 943m

[a] In CH_2Cl_2. [b] In Et_2O. [c] In tetrahydrofuran (thf). [d] In ethyl acetate. [e] In hexane.

distances and angles are listed in Table 2. The molecule possesses a crystallographically imposed two-fold axis bisecting the Os(3)–Os(3′), Os(1)–Os(1′), and Os(2)–Os(2′) edges. The metal-core geometry may be regarded as a Pt-bicapped osmium tetrahedron which is linked to a second osmium tetrahedron through a common edge, Os(1)–Os(1′). There are 16 carbonyl ligands; both Os(1) and Os(1′) possess two carbonyl ligands while each of the remaining Os atoms has three terminal carbonyl ligands. The mean Os–C and C–O bond distances are 1.90(3) and 1.15(2) Å, respectively, and the average Os–C–O angle is 176(2)°; these values are typical for linear carbonyls. Relatively close Pt···C(carbonyl) contacts are observed [Pt···C(21) 2.89(2), Pt···C(23) 3.03(2) Å], however this is probably caused by crystal packing effects and is not ascribed to incipient dihapto co-ordination of carbonyl ligands on the platinum atoms. The two C_8H_{12} ligands are each chelated to a Pt atom with the Pt–C distances, the Pt–C–C angles, and the distances and angles within the C_8H_{12} ligands falling within the ranges that have been previously observed in '$Pt(C_8H_{12})$' fragments.[8] The C=C bond lengths in the C_8H_{12} ligand are not equivalent (3.5 σ). This may be due to an underestimation of the errors or it could be related to the variations in the Os–Pt distances [Os(1)–Pt 2.624(1), Os(2)–Pt 2.805(1), and Os(2′)–Pt 2.901(1) Å] as the longest C=C bond, C(1)–C(2), is *trans* to the shortest Os–Pt separation, Os(1)–Pt. Unsymmetrical Pt capping atoms are also observed in compound (**1**) and the tetrahedral mixed-metal clusters $[PtOs_3(CO)_8(PMe_2Ph)(\mu_3\text{-}S)]$[9] and $[PtOs_3H_2(CO)_{10}\{P(C_6H_{11})_3\}]$.[10]

As discussed in the preliminary communication[3] the cluster (**2**) is a 108-electron system although it has the same metal-core geometry as the osmium anion $[Os_8H(CO)_{22}]^-$, which is a 110-electron system.[11] The structure of $[Os_8H(CO)_{22}]^-$ could not be predicted by conventional skeletal electron-counting procedures but it can be rationalized by the condensed polyhedral approach.[12] Neither of the two aforementioned methods nor the topological electron-counting scheme[13] are in agreement with the structure of (**2**).

A comparison of the metal–metal distances in (**2**) and $[Os_8H(CO)_{22}]^-$ reveals some interesting differences.[11] The dimensions associated with the bicapped tetrahedron appear normal,[14] as does the Os(1)–Os(3) distance. Thus the capping $Pt(C_8H_{12})$ units do not introduce any major perturbations into the metal core geometry. In (**2**) the Os(3)–Os(3′) distance, 2.647(1) Å, is abnormally short while the value reported for the corresponding distance in the Os cluster anion $[Os_8H(CO)_{22}]^-$, 2.848(1) Å, is a more typical Os–Os bond length. This short contact is in agreement with an Os(3)–Os(3′) double bond which must be formally assigned to this edge if the metals are to achieve an 18-electron configuration.

The conclusion that (**2**) is an electronically unsaturated cluster is supported by the observed reactivity. Solutions of (**2**) react immediately with carbon monoxide, in CH_2Cl_2 at 23 °C, to give (**1**) in 60% yield together with another product, yet uncharacterized. The reaction is somewhat reversible as reflux of (**1**) in octane affords (**2**) in 50% yield after 5 min (Figure 2).

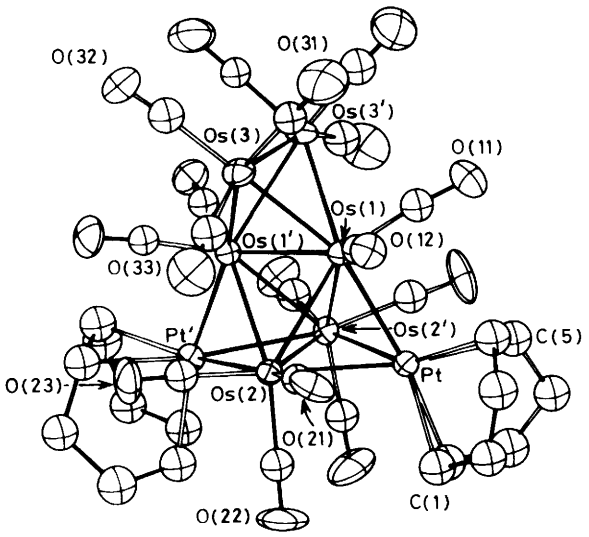

Figure 1. The molecular structure of $[Os_6Pt_2(CO)_{16}(C_8H_{12})_2]$ (**2**)

This type of rearrangement of the metallic core from a fused tetrahedron to a bicapped octahedron was also observed in homometallic Os_8 carbonyl clusters,[11] where deprotonation of $[Os_8H(CO)_{22}]^-$ gives $[Os_8(CO)_{22}]^{2-}$.

The presence of different metallic centres in clusters provides a probe for the investigation of metal-core rearrangements. The two Pt units capping opposite faces of one of the edge-fused tetrahedra in cluster (**2**) are found to be capping opposite faces of the octahedron in cluster (**1**) upon reversible carbonylation. Preliminary results obtained from extended-Hückel molecular orbital calculations[15] performed on the mixed-metal cluster (**2**) indicate a relatively strong antibonding interaction in the lowest unoccupied molecular orbital between the atoms Os(1) and Os(1′) (the common edge of the fused tetrahedra). Therefore, addition of a two-electron donor ligand should provoke the elongation of that edge. However, if only that occurred the capping Pt atoms would end up on adjacent faces of the octahedron instead of being on opposite faces as seen in (**1**). This clearly indicates a more complicated pathway for the rearrangement of the metal-core geometry. In order to gain information about the site of carbonyl attack on cluster (**2**), a different ligand was used: $P(OMe)_3$ was chosen because its bonding properties, a good σ-donor and π-acceptor ligand, are similar to those of CO.

A solution of $P(OMe)_3$ in CH_2Cl_2 was slowly added to (**2**), also dissolved in CH_2Cl_2, at 0 °C until qualitative t.l.c. indicated that all of (**2**) had reacted. Only one product (**3**) was obtained and recrystallization from Et_2O–CH_2Cl_2 at 0 °C yielded dark brown *X*-ray quality crystals. Figure 3 shows a perspective view of the unexpected mixed-metal cluster $[Os_6Pt_2(CO)_{16}(C_8H_{12})\{P(OMe)_3\}_2]$ (**3**) and Table 3 contains internuclear distances and angles. Interestingly, instead of adding the $P(OMe)_3$ to the metallic core, one of the Pt-bound C_8H_{12} ligands was substituted by two $P(OMe)_3$ groups. The reaction was carefully repeated, however no other product other than (**3**) was observed by t.l.c. during the addition of the $P(OMe)_3$ solution. Furthermore, exactly two equivalents of phosphite are needed to consume all of the starting material.

This new cluster (**3**) can be regarded as a bicapped tetrahedron of six Os atoms having two faces Pt-capped. The C_8H_{12} ligand is chelated to the Pt atom capping the central Os tetrahedron and the two $P(OMe)_3$ groups are bound to the Pt atom capping a face of one of the $Os(CO)_3$ capping units. Os(4) is the common vertex for both Pt fragments. All of the 16

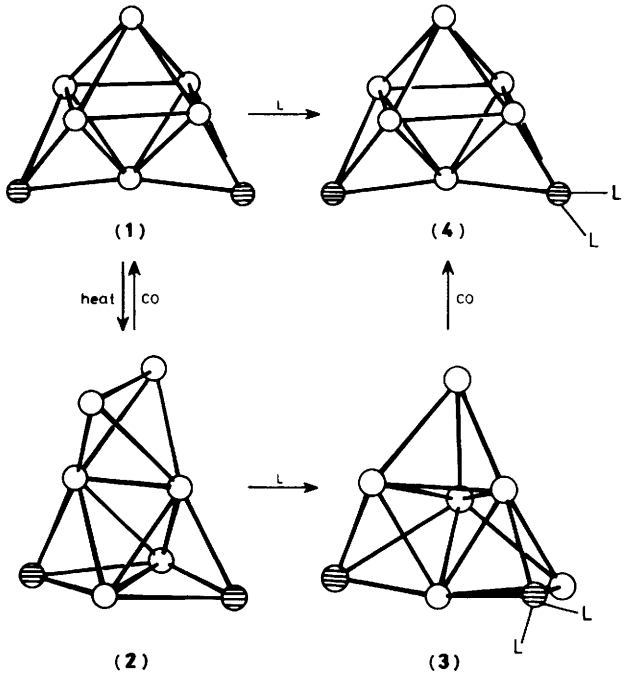

Figure 2. Some reactions of Os–Pt clusters showing the transformations between cluster cores of (**1**), (**2**), (**3**), and (**4**). The Pt atoms are shaded; L = $P(OMe)_3$

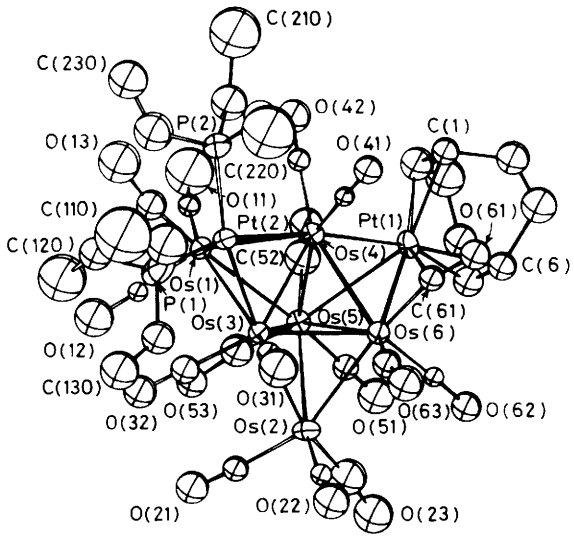

Figure 3. The molecular structure of $[Os_6Pt_2(CO)_{16}(C_8H_{12})\{P(OMe)_3\}_2]$ (**3**)

carbonyl ligands are linear and terminal except C(61)–O(61) [Os(6)–C(61)–O(61) 163(4)°], which semi-bridges the Os(6)–Pt(1) edge. The Os(6)–C(61) and Pt(1)–C(61) distances are 1.81(5) and 2.36(5) Å respectively. Os(4) and Os(3) each have two carbonyl ligands while the other four Os atoms are bonded to three carbonyls. A significant variation is observed in the Os–C and C–O distances [Os–C 1.62(5)—1.99(5) and C–O 1.09(5)—1.35(6) Å]; this is not without precedent, however, another example being the homometallic anion[16] $[Os_{10}C(CO)_{24}(\mu\text{-NO})]^-$. This variation may simply reflect the polarity of the molecule (**3**).

Table 2. Selected internuclear distances (Å) and angles (°) for $[Os_6Pt_2(CO)_{16}(C_8H_{12})_2]$ (**2**)*

Pt–Os(1)	2.624(1)	Os(2)–C(22)	1.913(15)	Pt–Os(2)	2.805(1)	Os(2)–C(23)	1.898(16)
Pt–Os(2′)	2.901(1′)	Os(3)–Os(3′)	2.647(1)	Pt–C(1)	2.315(15)	Os(3)–C(31)	1.859(15)
Pt–C(2)	2.263(16)	Os(3)–C(32)	1.884(17)	Pt–C(5)	2.240(17)	Os(3)–C(33)	1.925(16)
Pt–C(6)	2.214(17)	C(11)–O(11)	1.178(17)	Os(1)–Os(1′)	2.537(1)	C(12)–O(12)	1.115(15)
Os(1)–Os(2)	2.831(1)	C(21)–O(21)	1.129(15)	Os(1)–Os(2′)	2.807(1)	C(22)–O(22)	1.137(17)
Os(1)–Os(3)	2.872(1)	C(23)–O(23)	1.163(17)	Os(1)–Os(3′)	2.768(1)	C(31)–O(31)	1.167(18)
Os(1)–C(11)	1.870(15)	C(32)–O(32)	1.130(19)	Os(1)–C(12)	1.928(13)	C(33)–O(33)	1.149(17)
Os(2)–Os(2′)	2.708(1)	C(1)–C(2)	1.429(18)	Os(2)–C(21)	1.913(14)	C(5)–C(6)	1.333(20)
Os(1)–Pt–Os(2)	62.74(2)	Pt–Os(2)–Os(1′)	104.06(2)	Os(1)–Pt–Os(2′)	60.81(2)	Pt–Os(2)–Os(2′)	63.47(2)
Os(2)–Pt–Os(2′)	56.64(2)	Pt′–Os(2)–Os(1)	101.03(2)	Pt–Os(1)–Os(1′)	117.99(2)	Pt′–Os(2)–Os(1′)	54.71(2)
Pt–Os(1)–Os(2)	61.76(2)	Pt′–Os(2)–Os(2′)	59.89(2)	Pt–Os(1)–Os(2′)	64.48(2)	Os(1)–Os(2)–Os(1′)	53.49(2)
Pt–Os(1)–Os(3)	149.05(2)	Os(1)–Os(2)–Os(2′)	60.85(2)	Pt–Os(1)–Os(3′)	154.83(2)	Os(1′)–Os(2)–Os(2′)	61.73(2)
Os(1′)–Os(1)–Os(2)	62.77(2)	Os(1)–Os(3)–Os(1′)	53.43(2)	Os(1′)–Os(1)–Os(2′)	63.73(2)	Os(1)–Os(3)–Os(3′)	60.03(2)
Os(1′)–Os(1)–Os(3)	61.17(2)	Os(1′)–Os(3)–Os(3′)	64.03(2)	Os(1′)–Os(1)–Os(3′)	65.39(2)	Os(1)–C(11)–O(11)	175(1)
Os(2)–Os(1)–Os(2′)	57.42(2)	Os(1)–C(12)–O(12)	177(1)	Os(2)–Os(1)–Os(3)	96.85(2)	Os(2)–C(21)–O(21)	176(1)
Os(2)–Os(1)–Os(3′)	128.16(2)	Os(2)–C(22)–O(22)	179(1)	Os(2′)–Os(1)–Os(3)	124.90(2)	Os(2)–C(23)–O(23)	176(1)
Os(2′)–Os(1)–Os(3′)	99.87(2)	Os(3)–C(31)–O(31)	176(1)	Os(3)–Os(1)–Os(3′)	55.94(2)	Os(3)–C(32)–O(32)	176(2)
Pt–Os(2)–Pt′	122.75(2)	Os(3)–C(33)–O(33)	176(2)	Pt–Os(2)–Os(1)	55.50(2)		

* Estimated standard deviations in the least significant figure(s) are given in parentheses in this and all subsequent tables.

Table 3. Selected internuclear distances (Å) and angles (°) for $[Os_6Pt_2(CO)_{16}(C_8H_{12})\{P(OMe)_3\}_2]$ (**3**)

Pt(1)–Os(4)	2.647(3)	Os(5)–Os(6)	2.818(3)	Pt(1)–Os(5)	3.083(3)	Os(4)–C(42)	1.87(5)
Pt(1)–Os(6)	2.703(3)	Os(5)–C(52)	1.97(7)	Pt(1)–C(1)	2.28(5)	Os(5)–C(51)	1.81(5)
Pt(1)–C(2)	2.16(6)	Os(6)–C(61)	1.81(5)	Pt(1)–C(5)	2.30(5)	Os(5)–C(53)	1.73(6)
Pt(1)–C(6)	2.25(5)	Os(6)–C(63)	1.73(6)	Pt(1)–C(61)	2.36(5)	Os(6)–C(62)	1.80(4)
Pt(2)–Os(1)	2.930(3)	P(1)–O(120)	1.47(3)	Pt(2)–Os(3)	2.667(3)	P(1)–O(110)	1.56(5)
Pt(2)–Os(4)	2.836(3)	P(2)–O(210)	1.58(4)	Pt(2)–P(1)	2.22(2)	P(1)–O(130)	1.56(4)
Pt(2)–P(2)	2.23(1)	P(2)–O(230)	1.58(4)	Os(1)–Os(3)	2.761(3)	P(2)–O(220)	1.54(4)
Os(1)–Os(4)	2.698(3)	O(12)–C(12)	1.19(5)	Os(1)–Os(5)	3.014(3)	O(11)–C(11)	1.15(6)
Os(1)–C(11)	1.99(5)	O(21)–C(21)	1.091(5)	Os(1)–C(12)	1.81(4)	O(13)–C(13)	1.32(6)
Os(1)–C(13)	1.62(5)	O(23)–C(23)	1.32(7)	Os(2)–Os(3)	2.685(3)	O(22)–C(22)	1.20(6)
Os(2)–Os(5)	2.936(3)	O(32)–C(32)	1.14(5)	Os(2)–Os(6)	2.804(3)	O(31)–C(31)	1.24(6)
Os(2)–C(21)	1.88(5)	O(42)–C(42)	1.10(5)	Os(2)–C(22)	1.79(5)	O(41)–C(41)	1.28(5)
Os(2)–C(23)	1.74(6)	O(52)–C(52)	1.14(7)	Os(3)–Os(4)	2.659(3)	O(51)–C(51)	1.18(5)
Os(3)–Os(5)	2.782(3)	O(61)–C(61)	1.19(5)	Os(3)–Os(6)	2.765(2)	O(53)–C(53)	1.29(6)
Os(3)–C(31)	1.77(5)	O(63)–C(63)	1.35(6)	Os(3)–C(32)	1.86(5)	O(62)–C(62)	1.20(4)
Os(4)–Os(5)	2.865(3)	C(5)–C(6)	1.35(7)	Os(4)–Os(6)	2.738(2)	C(1)–C(2)	1.34(7)
Os(4)–C(41)	1.71(4)						
Os(4)–Pt(1)–Os(5)	59.41(7)	Os(5)–Os(4)–Os(6)	60.35(7)	Os(4)–Pt(1)–Os(6)	61.54(7)	Os(1)–Os(5)–Os(2)	108.18(8)
Os(5)–Pt(1)–Os(6)	57.84(7)	Os(1)–Os(5)–Os(3)	56.72(6)	Os(1)–Pt(2)–Os(3)	58.89(7)	Os(1)–Os(5)–Os(4)	54.57(6)
Os(1)–Pt(2)–Os(4)	55.76(6)	Os(1)–Os(5)–Os(6)	103.69(8)	Os(3)–Pt(2)–Os(4)	57.70(7)	Os(2)–Os(5)–Os(3)	55.93(7)
Pt(2)–Os(1)–Os(3)	55.79(6)	Os(2)–Os(5)–Os(4)	102.35(9)	Pt(2)–Os(1)–Os(4)	60.34(7)	Os(2)–Os(5)–Os(6)	58.28(7)
Pt(2)–Os(1)–Os(5)	105.86(7)	Os(3)–Os(5)–Os(4)	56.17(7)	Os(3)–Os(1)–Os(4)	58.30(7)	Os(3)–Os(5)–Os(6)	59.17(7)
Os(3)–Os(1)–Os(5)	57.40(6)	Os(4)–Os(5)–Os(6)	57.59(6)	Os(4)–Os(1)–Os(5)	59.90(6)	Pt(1)–Os(6)–Os(2)	127.7(1)
Os(3)–Os(2)–Os(5)	59.13(7)	Pt(1)–Os(6)–Os(3)	110.11(8)	Os(3)–Os(2)–Os(6)	60.45(7)	Pt(1)–Os(6)–Os(4)	58.23(7)
Os(5)–Os(2)–Os(6)	58.75(7)	Pt(1)–Os(6)–Os(5)	67.86(7)	Pt(2)–Os(3)–Os(1)	65.33(7)	Os(2)–Os(6)–Os(3)	57.64(7)
Pt(2)–Os(3)–Os(2)	169.4(1)	Os(2)–Os(6)–Os(4)	109.28(8)	Pt(2)–Os(3)–Os(4)	64.34(7)	Os(2)–Os(6)–Os(5)	62.97(7)
Pt(2)–Os(3)–Os(5)	121.02(9)	Os(3)–Os(6)–Os(4)	57.80(6)	Pt(2)–Os(3)–Os(6)	111.97(9)	Os(3)–Os(6)–Os(5)	59.77(7)
Os(1)–Os(3)–Os(2)	124.5(1)	Os(4)–Os(6)–Os(5)	62.06(7)	Os(1)–Os(3)–Os(4)	59.67(7)	Pt(2)–P(1)–O(110)	113(2)
Os(1)–Os(3)–Os(5)	65.88(7)	Pt(2)–P(1)–O(120)	119(2)	Os(1)–Os(3)–Os(6)	112.24(9)	Pt(2)–P(1)–O(130)	112(2)
Os(2)–Os(3)–Os(4)	115.49(9)	Pt(2)–P(2)–O(210)	109(2)	Os(2)–Os(3)–Os(5)	64.94(8)	Pt(2)–P(2)–O(220)	122(2)
Os(2)–Os(3)–Os(6)	61.91(7)	Pt(2)–P(2)–O(230)	114(2)	Os(4)–Os(3)–Os(5)	63.48(7)	Os(1)–C(11)–O(11)	166(5)
Os(4)–Os(3)–Os(6)	60.58(7)	Os(1)–C(12)–O(12)	170(4)	Os(5)–Os(3)–Os(6)	61.06(7)	Os(1)–C(13)–O(14)	169(5)
Pt(1)–Os(4)–Pt(2)	166.63(9)	Os(2)–C(21)–O(21)	175(4)	Pt(1)–Os(4)–Os(1)	125.0(1)	Os(2)–C(22)–O(22)	176(4)
Pt(1)–Os(4)–Os(3)	115.24(9)	Os(2)–C(23)–O(23)	173(6)	Pt(1)–Os(4)–Os(5)	67.89(7)	Os(3)–C(31)–O(31)	177(4)
Pt(1)–Os(4)–Os(6)	60.23(7)	Os(3)–C(32)–O(32)	173(5)	Pt(2)–Os(4)–Os(1)	63.89(7)	Os(4)–C(41)–O(41)	177(4)
Pt(2)–Os(4)–Os(3)	57.96(7)	Os(4)–C(42)–O(42)	175(4)	Pt(2)–Os(4)–Os(5)	112.63(8)	Os(5)–C(51)–O(51)	179(4)
Pt(2)–Os(4)–Os(6)	107.76(9)	Os(5)–C(52)–O(52)	172(5)	Os(1)–Os(4)–Os(3)	62.03(7)	Os(5)–C(53)–O(53)	167(5)
Os(1)–Os(4)–Os(5)	65.54(7)	Pt(1)–C(61)–O(61)	113(4)	Os(1)–Os(4)–Os(6)	115.12(9)	Os(6)–C(61)–O(61)	163(4)
Os(3)–Os(4)–Os(5)	60.34(7)	Os(6)–C(62)–O(62)	172(4)	Os(3)–Os(4)–Os(6)	61.61(7)	Os(6)–C(63)–O(63)	168(4)

There are no platinum–trimethyl phosphite complexes reported in the literature for comparisons of values; however, the average of the Pt–P distances, 2.224(8) Å, is exactly the same as that found for platinum–triphenyl phosphite in the compounds $[FePt_2(CO)_5\{P(OPh)_3\}_3]$[17] and $[\{Pt(SPEt_2)\text{-}[P(OPh)_3]\}_2]$.[18] The distances within the $P(OMe)_3$ ligands are comparable to those found in the homometallic clusters $[Os_3(CO)_{11}\{P(OMe)_3\}]$[19] and $[Os_5(CO)_{16}\{P(OMe)_3\}_3]$.[20] The bond parameters in the $Pt(C_8H_{12})$ fragment are comparable with those observed for (**2**).

The six Os atoms are arranged in a bicapped tetrahedral unit similar to the Os_6 core observed in $[Os_6(CO)_{18}]$[14] in which the

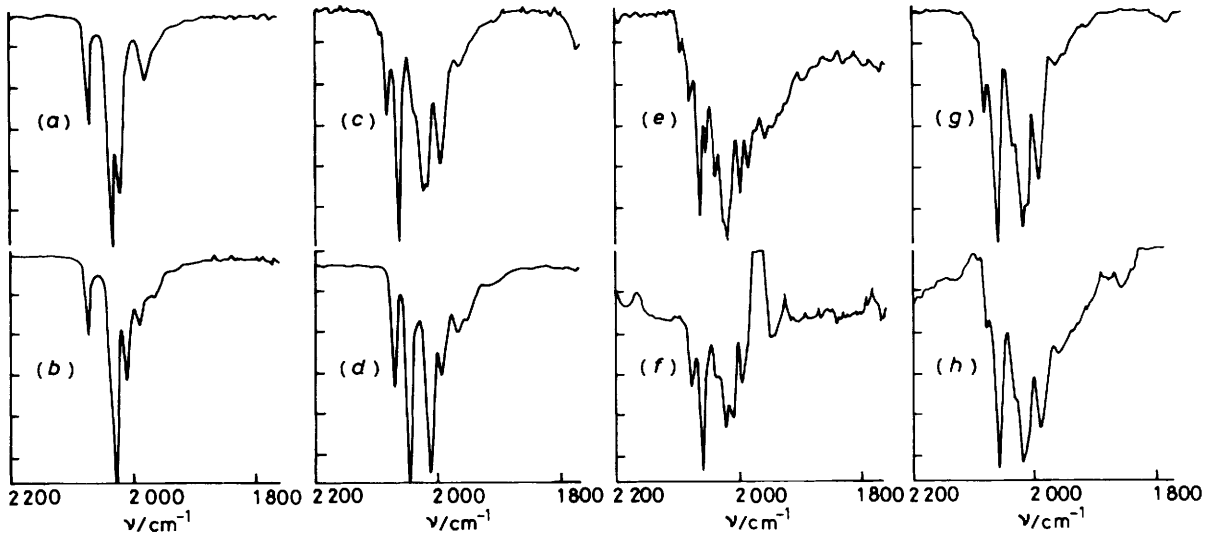

Figure 4. Infrared spectra (2 200—1 800 cm^{-1}), in CH_2Cl_2: (*a*) (**1**), (*b*) (**4**), (*c*) (**2**), (*d*) (**3**). Spectra for $[Os_6Pt_2(CO)_{16}(C_8H_{12})_2]$ (**2**) recorded in different solvents: (*e*) in hexane, (*f*) in Et_2O, (*g*) in thf, (*h*) in ethyl acetate

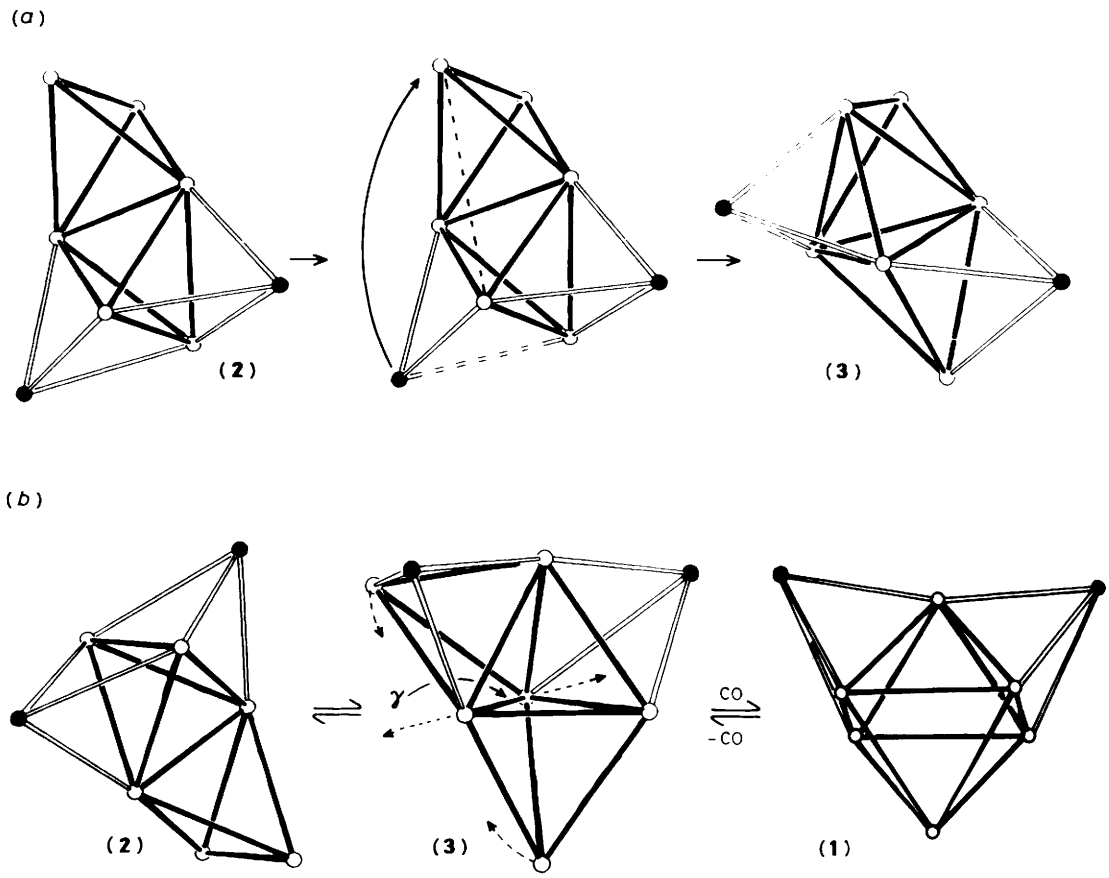

Figure 5. (*a*) Transformation from cluster (**2**) to cluster (**3**). (*b*) Transformation from cluster (**2**) to cluster (**1**). The Pt atoms are represented by the full circles

Os–Os distances vary from 2.731(1) to 2.836(1) Å. A large range is observed in cluster (**3**), where the shortest Os–Os separation is the edge Os(3)–Os(4), 2.659(3) Å, and the longest is Os(1)–Os(5), 3.014(3) Å. The Pt atoms unsymmetrically cap triangular osmium faces. One Os–Pt distance of the Pt–phosphite unit [Os(3)–Pt(2) 2.667(3) Å] is shorter than the other two [Os(1)–Pt(2) 2.930(3) and Os(4)–Pt(2) 2.836(3) Å]; this feature is also observed in (**2**). Interestingly, this trend is reversed in the $Pt(C_8H_{12})$ fragment of compound (**3**), one Os–Pt distance [Os(5)–Pt(1) 3.083(3) Å] is considerably longer than the other

two [Os(4)–Pt(1) 2.647(3) and Os(6)–Pt(1) 2.703(3) Å]. This type of variation in the Os–Pt distances, either one longer than the other two or one shorter than the other two, is present in all the high-nuclearity osmium–platinum clusters that we have structurally characterized.[3,5]

The cluster (**3**) is also a 108-electron system and in contrast to (**2**), its metallic framework is consistent with the skeletal electron-counting methods.

Cluster (**3**) reacts immediately with CO to afford quantitative yields of a new complex (**4**). The i.r. spectrum of complex (**4**) closely resembles that of (**1**), the Pt-bicapped octahedron. The addition of two equivalents of $P(OMe)_3$ to a solution of cluster (**1**) also gives the product (**4**), which is therefore formulated as $[Os_6Pt_2(CO)_{17}(C_8H_{12})\{P(OMe)_3\}_2]$ (**4**). The Pt-bicapped octahedral geometry appears to be the least reactive of all the mixed-metal clusters presented in this paper. The substitution of one C_8H_{12} ligand for two $P(OMe)_3$ groups is more facile with the Pt-bicapped edge-fused tetrahedron of (**2**) (immediately at 0 °C) than with the Pt-bicapped octahedron of (**1**) (16 h at 23 °C). Figure 2 illustrates the reactions and some of the i.r. spectra of the complexes are shown in Figure 4.

The transformation from cluster (**2**) to (**3**) is depicted in Figure 5(*a*). A subtle flexion at the common edge of the edge-fused tetrahedra brings two osmium atoms into interaction with the concerted slip of one Pt cap, the $Pt(C_8H_{12})$ fragment in this case, onto the new triangular face. This motion has to be accompanied by carbonyl migration in order to obtain the right co-ordination number for each of the six osmium atoms in cluster (**3**). This interconversion of cluster geometries may be occurring in solutions of (**2**). There is some evidence for structural non-rigidity as the i.r. spectra of (**2**) in certain solvents (Figure 4) strongly resemble that of the phosphite derivative (**3**).

Compound (**3**) reacts with CO to give a cluster having a bicapped octahedral geometry. This transformation can be obtained simply by moving apart the two Os atoms [*i.e.* Os(3) and Os(5) of cluster (**3**)], forming bond γ in structure (**3**) [Figure 5(*b*)], producing a Pt-bicapped octahedron similar to the metal core of (**1**), without migration of the platinum atoms. The metal core of (**3**) is therefore postulated as an intermediate for the formation of $[Os_6Pt_2(CO)_{17}(C_8H_{12})_2]$ (**1**) with a possible equilibrium between the core structures (**2**) and (**3**).

The rearrangement of a bicapped tetrahedron to an octahedron is observed with $[Os_6(CO)_{18}]$,[21] which reversibly transforms to an octahedron, $[Os_6(CO)_{18}]^{2-}$, upon addition of two electrons. This process of bond elongation and bond formation is analogous to the stretching of two common triangulated faces to a square face in borane cages,[22] a concept put forward to encompass rearrangements in borane polyhedra. At this point, further experiments need to be performed in order to examine the solution structures of the clusters. We are presently enriching these mixed-metal clusters with ^{13}CO in the hope that this will enable us to study their fluxional behaviour by ^{13}C n.m.r. spectroscopy.

Experimental

The compounds $[Os_6(CO)_{18}]$[23] and $[Pt(C_8H_{12})_2]$[24] were prepared by literature methods. All reactions were performed under nitrogen using dry, freshly distilled solvents. Me_3NO was sublimed and stored under N_2 prior to use. Silica gel (28—200 mesh) was used for filtration. Product separation was carried out, in air, using thin-layer chromatography (t.l.c.; plates 0.25-mm thickness, Merck Kieselgel 60); R_f values are not quoted since all the plates were continuously eluted until acceptable separation was achieved.

Infrared spectra were recorded on a Nicolet 5DX FTIR spectrophotometer. ^1H N.m.r. spectra were obtained on a Varian XL-200 spectrometer.

Preparations.—$[Os_6(CO)_{18-n}(NCMe)_n]$ (n = 1 *or* 2). In a typical reaction $[Os_6(CO)_{18}]$ (100 mg) was dissolved in CH_2Cl_2–MeCN (40:1; 41 cm^3). This solution was cooled to −78 °C using an acetone–dry ice bath. A solution of Me_3NO in CH_2Cl_2 (4.6 mg in 20 cm^3 for n = 1 or 9.2 mg in 40 cm^3 for n = 2) was then slowly added over a period of 40—80 min. The reaction mixture was then allowed to warm up to ambient temperature and filtered through silica gel to remove any excess of Me_3NO. The solvent was evaporated under vacuum and 40 cm^3 of pure CH_2Cl_2 were used to redissolve the red-brown solid. For subsequent reactions the acetonitrile complexes were used without further purification.

Reactions of $[Os_6(CO)_{18-n}(NCMe)_n]$ (n = 1 *or* 2) *with* $[Pt(C_8H_{12})_2]$.—Two equivalents of $[Pt(C_8H_{12})_2]$ {50 mg, based on $[Os_6(CO)_{18}]$ weight of 100 mg} were added to a frozen solution of $[Os_6(CO)_{18-n}(NCMe)_n]$ (n = 1 or 2) in CH_2Cl_2 (40 cm^3). The reaction mixtures were allowed to warm up to room temperature and stirred for 18 h. The solutions were then concentrated and the products separated by t.l.c., continuously eluting with hexane–CH_2Cl_2 (3:1). About 20% of the products did not move on the t.l.c. plate while the remainder generally separated into ten bands. Three or four major bands are generally observed: for n = 1 the mauve band (sixth from the top) is $[Os_6Pt_2(CO)_{17}(C_8H_{12})_2]$ (**1**) (yield 20%); for n = 2, the brown fifth band is $[Os_6Pt_2(CO)_{16}(C_8H_{12})_2]$ (**2**) (yield 15%). *X*-Ray quality crystals were obtained from the slow evaporation of an ethyl acetate solution.

Synthesis of $[Os_6Pt_2(CO)_{16}(C_8H_{12})\{P(OMe)_3\}_2]$ (**3**).—Addition of a CH_2Cl_2 solution containing two equivalents of $P(OMe)_3$ to $[Os_6Pt_2(CO)_{16}(C_8H_{12})_2]$ (**2**) (10 mg) in CH_2Cl_2 (20 cm^3) at −50 °C immediately gave the brown product $[Os_6Pt_2(CO)_{16}(C_8H_{12})\{P(OMe)_3\}_2]$ (**3**). The product was purified by t.l.c. using hexane–CH_2Cl_2 (1:1) as eluant, and recrystallized from Et_2O–CH_2Cl_2 at 0 °C (yield 95%).

Reaction of $[Os_6Pt_2(CO)_{17}(C_8H_{12})_2]$ (**1**) *in Octane under Reflux.*—$[Os_6Pt_2(CO)_{17}(C_8H_{12})_2]$ (**1**) (5 mg) was heated in octane (10 cm^3) under reflux for 30 min. The solvent was removed and the products were separated by t.l.c. using hexane–CH_2Cl_2 (3:1) as eluant. Approximately 40% of the products remained on the baseline, while $[Os_6Pt_2(CO)_{16}(C_8H_{12})_2]$ (**2**) was separated as the major product (yield 50%) with three other minor products.

Reaction of $[Os_6Pt_2(CO)_{16}(C_8H_{12})_2]$ (**2**) *with* CO.—Carbon monoxide was bubbled through a solution of $[Os_6Pt_2(CO)_{16}(C_8H_{12})_2]$ (**2**) (5 mg) in CH_2Cl_2 (5 cm^3) for 10 s at room temperature. T.l.c. of the solution using hexane–CH_2Cl_2 (4:1) as eluant gave only two major products: $[Os_6Pt_2(CO)_{17}(C_8H_{12})_2]$ (**1**) (yield 60%) and, above it, an uncharacterized red-brown product (yield 30%).

Reaction of $[Os_6Pt_2(CO)_{16}(C_8H_{12})\{P(OMe)_3\}_2]$ (**3**) *with* CO.—$[Os_6Pt_2(CO)_{16}(C_8H_{12})\{P(OMe)_3\}_2]$ (**3**) (5 mg) was dissolved in CH_2Cl_2 (5 cm^3), the solution was then frozen. Carbon monoxide (50 cm^3) was admitted into the evacuated reaction flask. The solid reaction mixture was allowed to warm up to ambient temperature and stirred for 5 min. The solvent and excess CO were removed under vacuum and t.l.c. of the red solid in hexane–CH_2Cl_2 (1:1) gave only one product, $[Os_6Pt_2(CO)_{17}(C_8H_{12})\{P(OMe)_3\}_2]$ (**4**), showing the same i.r. spectrum as the product from the reaction of $[Os_6Pt_2(CO)_{17}(C_8H_{12})_2]$ (**1**) with $P(OMe)_3$ (see below).

Reaction of $[Os_6Pt_2(CO)_{17}(C_8H_{12})_2]$ (**1**) *with* $P(OMe)_3$.—$[Os_6Pt_2(CO)_{17}(C_8H_{12})_2]$ (**1**) (5 mg) was dissolved in CH_2Cl_2

Table 4. Positional parameters for the non-H atoms of $[Os_6Pt_2(CO)_{16}(C_8H_{12})_2]$ (**2**)

Atom	*x*	*y*	*z*	Atom	*x*	*y*	*z*
Pt	−0.123 24(3)	0.039 12(4)	0.145 75(3)	C(3)	−0.208 3(9)	−0.155(2)	0.169 2(9)
Os(1)	−0.063 49(3)	0.237 06(4)	0.200 8(3)	C(4)	−0.263 6(8)	−0.058(1)	0.132 2(9)
Os(2)	0.184 3(3)	0.055 43(4)	0.183 93(3)	C(5)	−0.234 6(8)	0.057(1)	0.123 6(9)
Os(3)	0.0224 8(3)	0.420 51(5)	0.189 18(3)	C(6)	−0.226 8(8)	0.094(1)	0.055 4(9)
O(11)	−0.194 2(5)	0.317(1)	0.217 6(6)	C(7)	−0.239(1)	0.030(2)	−0.024(1)
O(12)	−0.123 7(5)	0.306 6(9)	0.016 6(5)	C(8)	−0.219 6(9)	−0.092(1)	−0.014 7(9)
O(21)	−0.055 3(6)	0.092 5(9)	−0.004 7(5)	C(11)	−0.142 4(7)	0.291(1)	0.212 5(8)
O(22)	0.021 7(7)	−0.203 8(9)	0.164 8(7)	C(12)	−0.102 1(7)	0.284(1)	0.084 8(8)
O(23)	0.154 1(5)	0.096(1)	0.164 7(6)	C(21)	−0.029 5(7)	0.082(1)	0.065 8(8)
O(31)	−0.089 2(7)	0.592(1)	0.095 9(7)	C(22)	0.020 7(7)	−0.107(1)	0.171 0(8)
O(32)	0.135 7(7)	0.597(1)	0.241 4(9)	C(23)	0.103 2(8)	0.083(1)	0.174 2(8)
O(33)	0.056 3(7)	0.317(1)	0.047 8(6)	C(31)	−0.045 3(7)	0.526(1)	0.129 2(8)
C(1)	−0.155 2(8)	−0.120(1)	0.059 6(8)	C(32)	0.091 8(8)	0.534(1)	0.222 2(9)
C(2)	−0.151 4(8)	−0.148(1)	0.141 4(8)	C(33)	0.044 0(9)	0.359(1)	0.099 8(9)

Table 5. Positional parameters for the non-H atoms of $[Os_6Pt_2(CO)_{16}(C_8H_{12})\{P(OMe)_3\}_2]$ (**3**)

Atom	*x*	*y*	*z*	Atom	*x*	*y*	*z*
Pt(1)	0.121 6(1)	0.273 9(2)	0.647 6(1)	O(230)	0.380(3)	−0.281(4)	0.759(2)
Pt(2)	0.337 4(1)	−0.054 1(2)	0.665 0(1)	C(1)	0.081(4)	0.256(5)	0.742(3)
Os(1)	0.204 2(2)	−0.104 0(2)	0.579 8(1)	C(2)	0.036(4)	0.209(6)	0.694(3)
Os(2)	0.265 3(2)	0.260 8(2)	0.474 7(1)	C(3)	−0.041(5)	0.268(7)	0.657(4)
Os(3)	0.293 5(1)	0.087 3(2)	0.564 3(1)	C(4)	−0.031(4)	0.353(6)	0.605(3)
Os(4)	0.214 8(1)	0.093 8(2)	0.656 2(1)	C(5)	0.038(4)	0.410(6)	0.600(3)
Os(5)	0.150 7(1)	0.139 9(2)	0.527 1(1)	C(6)	0.077(4)	0.464(5)	0.651(3)
Os(6)	0.242 0(1)	0.308 5(2)	0.599 1(1)	C(7)	0.053(4)	0.476(6)	0.720(4)
P(1)	0.435(1)	−0.144(2)	0.646(1)	C(8)	0.074(4)	0.387(6)	0.765(4)
P(2)	0.344(1)	−0.152(1)	0.757 7(8)	C(11)	0.107(3)	−0.173(5)	0.572(3)
O(11)	0.053(4)	−0.208(6)	0.581(3)	C(12)	0.206(3)	−0.184(4)	0.506(2)
O(12)	0.218(3)	−0.242(4)	0.461(3)	C(13)	0.230(4)	−0.233(5)	0.612(3)
O(13)	0.248(3)	−0.330(5)	0.648(3)	C(21)	0.274(4)	0.163(5)	0.404(3)
O(21)	0.281(3)	0.100(4)	0.366(2)	C(22)	0.349(3)	0.335(4)	0.476(3)
O(22)	0.406(3)	0.384(4)	0.481(2)	C(23)	0.223(5)	0.377(7)	0.427(4)
O(23)	0.188(3)	0.454(4)	0.386(3)	C(31)	0.382(3)	0.133(4)	0.590(2)
O(31)	0.443(3)	0.170(4)	0.609(3)	C(32)	0.317(4)	−0.015(5)	0.501(3)
O(32)	0.337(3)	−0.079(4)	0.466(2)	C(41)	0.261(3)	0.123(4)	0.730(3)
O(41)	0.294(2)	0.148(3)	0.786(2)	C(42)	0.153(3)	−0.005(5)	0.694(3)
O(42)	0.117(3)	−0.057(4)	0.719(2)	C(51)	0.104(4)	0.263(5)	0.482(3)
O(51)	0.074(3)	0.345(4)	0.454(2)	C(52)	0.063(5)	0.081(6)	0.554(4)
O(52)	0.009(3)	0.054(4)	0.564(2)	C(53)	0.137(4)	0.048(6)	0.461(3)
O(53)	0.139(3)	−0.007(4)	0.407(2)	C(61)	0.235(4)	0.359(5)	0.679(3)
O(61)	0.240(3)	0.417(4)	0.726(2)	C(62)	0.204(3)	0.447(4)	0.564(3)
O(62)	0.174(3)	0.532(3)	0.535(2)	C(63)	0.329(4)	0.359(5)	0.613(3)
O(63)	0.391(3)	0.416(4)	0.631(2)	C(110)	0.546(8)	−0.23(1)	0.717(7)
O(110)	0.495(3)	−0.146(5)	0.705(3)	C(120)	0.398(6)	−0.320(8)	0.571(5)
O(120)	0.433(3)	−0.276(4)	0.631(2)	C(130)	0.528(5)	−0.118(7)	0.568(4)
O(130)	0.467(3)	−0.080(4)	0.591(2)	C(210)	0.237(7)	−0.23(1)	0.832(5)
O(210)	0.266(3)	−0.175(4)	0.772(2)	C(220)	0.439(7)	−0.06(1)	0.843(6)
O(220)	0.372(3)	−0.091(4)	0.822(2)	C(230)	0.388(5)	−0.374(7)	0.804(4)

(10 cm^3), then less than two equivalents of $P(OMe)_3$ (0.3 mg) in CH_2Cl_2 (5 cm^3) were slowly added to the solution at ambient temperature. The reaction mixture was stirred for 18 h and the solvent removed under vacuum. The t.l.c. plate [using hexane–CH_2Cl_2 (1:1) as eluant] showed only two compounds: the upper mauve band was unreacted $[Os_6Pt_2(CO)_{17}(C_8H_{12})_2]$ (**1**) (yield 40%) and the red lower band, $[Os_6Pt_2(CO)_{17}(C_8H_{12})\{P(OMe)_3\}_2]$ (**4**) (yield 60%), having the same i.r. spectrum as the product from the reaction of $[Os_6Pt_2(CO)_{16}(C_8H_{12})\{P(OMe)_3\}_2]$ (**3**) with CO.

Crystal Data for (**2**).—$C_{32}H_{24}O_{16}Os_6Pt_2$, M = 2 195.92, monoclinic, a = 21.178(3), b = 11.683(2), c = 17.383(2) Å, β = 113.83(1)°, U = 3 934.1 Å^3 (by least-squares refinements on diffractometer angles for 25 automatically centred reflections, λ = 0.710 69 Å), space group $C2/c$, Z = 4, D_c = 3.75 g cm^{-3}, $F(000)$ = 3 824. Dark brown plates, crystal dimensions 0.037 × 0.105 × 0.237 mm, crystal faces {100}, {010}, {001}, {011}, μ(Mo-K_α) = 265.5 cm^{-1}.

Crystal Data for (**3**).—$C_{30}H_{30}O_{22}Os_6P_2Pt_2$, M = 2 335.90, monoclinic, a = 19.160(4), b = 10.963(2), c = 21.277(6) Å, β = 99.40(2)°, U = 4 409.2 Å^3 (by least-squares refinements on diffractometer angles for 22 automatically centred reflections, λ = 0.710 69 Å), space group $P2_1/c$, Z = 4, D_c = 3.19 g cm^{-3}, $F(000)$ = 4 112. Dark brown plates, crystal dimensions 0.056 × 0.104 × 0.128 mm, crystal faces {100}, {001}, {$\bar{1}$11}, μ(Mo-K_α) = 237.4 cm^{-1}.

Data Collection and Processing.[25]—Enraf-Nonius CAD4 diffractomer, θ/2θ mode with scan width = 0.75 + 0.35 tanθ, scan speed 1.0—11.0° min^{-1}, graphite-monochromated Mo-K_α

radiation; for (**2**), a photographic examination showed the crystals belonged to one of the monoclinic space groups *Cc* or *C*2/*c*. An examination of *X*-ray intensities following data collection strongly suggested a centrosymmetric structure and the chosen space group *C*2/*c* was confirmed by a successful analysis. 3 555 Unique reflections measured ($2 \leqslant 2\theta \leqslant 45°$, $+h, +k, \pm l$), azimuthal scan data for eight reflections were used in the empirical absorption correction (max., min. correction factors = 1.0000, 0.3998) giving 2 679 with $I > 3\sigma(I)$. No decay was observed. For (**3**) several ω-scans of intense, low-angle reflections indicated that the crystals were barely of adequate mosaicity. 5 876 Unique reflections measured ($2 \leqslant 2\theta \leqslant 40°$, $+h, +k, \pm l$), Gaussian absorption correction with a grid of 4 × 14 × 8 (transmission coefficients from 0.021 to 0.303), giving 2 929 with $I > 3\sigma(I)$. Crystal decay, *ca.* 5.6%, corrected during processing.

Structure Analysis and Refinement.—Both structures were solved by automatic direct methods and followed by difference Fourier syntheses.

Structure (**2**) was refined with Os, Pt, and O atoms assigned anisotropic thermal parameters and the C atoms individual isotropic thermal parameters. H Atoms were located in a difference Fourier synthesis and they were included in subsequent calculations with idealized positional co-ordinates (either sp^2 or sp^3 geometry and C–H bond distance of 0.95 Å) but were not refined. The refinement converged at $R = \Sigma(||F_o| - |F_c||)/\Sigma|F_o| = 0.044$ and $R' = \Sigma w(|F_o| - |F_c|)^2 = 0.034$, where the weight $w = 4F_o^2/\sigma^2(F_o^2)$ (2 675 observations and 173 variables). In the final cycle no shift exceeded 0.16 of its standard deviation. A total difference Fourier synthesis calculated from the final structure factors contained no features of chemical significance with the highest peak, of electron density 2.4 e Å^{-3}, at fractional co-ordinates (−0.029, 0.063, 0.167) associated with Pt.

Structure (**3**) was refined with Os, Pt, and P atoms assigned anisotropic thermal parameters and the C and O atoms individual isotropic thermal parameters. Hydrogen atoms were not located due to the poor quality of the data (poor crystal mosaicity) but were included in the final calculations with idealized positional co-ordinates (sp^3 geometry and C–H bond distance of 0.95 Å; the ethylenic H were excluded) but not refined. The refinement converged at $R = 0.086$ and $R' = 0.073$, where the weight $w = 4F_o^2/\sigma^2(F_o^2)$ (2 818 observations and 299 variables). In the final cycle no shift exceeded 0.07 of its standard deviation. A total difference Fourier synthesis calculated from the final structure factors contained no features of chemical significance with the highest peak, of electron density 4.4 e Å^{-3}, at fractional co-ordinates (0.203, 0.000, 0.572) associated with Os(6).

Complex neutral-atom scattering factors [26] were employed in both structure solutions and refinements. All computations were performed on a DEC PDP-11/23 computer at the University of Toronto using the SDP-Plus system.[25] The molecular plots were drawn using the program ORTEP.[27] Final position parameters for the non-H atoms for complexes (**2**) and (**3**) are given in Tables 4 and 5.

Acknowledgements

We are grateful to Professor Roald Hoffmann and Dr. Chong Zheng for their assistance in performing the extended-Hückel molecular orbital calculations on compound (**2**). We thank the Natural Sciences and Engineering Research Council of Canada for operating grants and major equipment grants and for a scholarship (to C. C.).

References

1 J. N. Nicholls, D. H. Farrar, P. F. Jackson, B. F. G. Johnson, and J. Lewis, *J. Chem. Soc., Dalton Trans.*, 1982, 1395.
2 W. L. Gladfelter and G. L. Geoffroy, *Adv. Organomet. Chem.*, 1980, **18**, 207.
3 C. Couture and D. H. Farrar, *J. Chem. Soc., Chem. Commun.*, 1985, 197.
4 M. P. Gomez-Bal, B. F. G. Johnson, R. A. Kamarudin, J. Lewis, P. R. Raithby, C. Couture, and D. H. Farrar, *Acta Crystallogr., Sect. C*, 1986, **42**, 163.
5 C. Couture, D. H. Farrar, and R. J. Goudsmit, *Inorg. Chim. Acta*, 1984, **89**, L29.
6 K. Wade, *Chem. Commun.*, 1971, 792.
7 P. F. Jackson, B. F. G. Johnson, J. Lewis, and P. R. Raithby, *J. Chem. Soc., Chem. Commun.*, 1980, 60.
8 M. Green, J. A. K. Howard, A. Laguna, L. E. Smart, J. L. Spencer, and F. G. A. Stone, *J. Chem. Soc., Dalton Trans.*, 1977, 278; G. K. Barker, M. Green, J. A. K. Howard, J. L. Spencer, and F. G. A. Stone, *ibid.*, 1978, 1839; A. B. Goel, and D. Van Der Veer, *Inorg. Chim. Acta*, 1982, **65**, L205; J. A. K. Howard, *Acta Crystallogr., Sect. B*, 1982, **38**, 2896.
9 R. D. Adams, T. S. A. Hor, and P. Mathur, *Organometallics*, 1984, **3**, 634.
10 L. J. Farrugia, M. Green, D. R. Hankey, M. Murray, A. G. Orpen, and F. G. A. Stone, *J. Chem. Soc., Dalton Trans.*, 1985, 177.
11 B. F. G. Johnson, J. Lewis, W. J. H. Nelson, M. D. Vargas, D. Braga, K. Henrick, and M. McPartlin, *J. Chem. Soc., Dalton Trans.*, 1984, 2151.
12 D. M. P. Mingos, *Acc. Chem. Res.*, 1984, **17**, 311.
13 B. K. Teo, *Inorg. Chem.*, 1984, **23**, 1251.
14 R. Mason, K. M. Thomas, and D. M. P. Mingos, *J. Am. Chem. Soc.*, 1973, **95**, 3802.
15 C. Couture, and D. H. Farrar, unpublished work.
16 B. F. G. Johnson, J. Lewis, W. J. H. Nelson, and J. Puga, *J. Organomet. Chem.*, 1984, **266**, 173.
17 V. G. Albino and G. Ciani, *J. Organomet. Chem.*, 1974, **66**, 311.
18 K. P. Wagner, R. W. Hess, P. M. Treichel, and J. C. Calabrese, *Inorg. Chem.*, 1975, **14**, 1121.
19 R. E. Benfield, B. F. G. Johnson, P. R. Raithby, and G. M. Sheldrick, *Acta Crystallogr., Sect. B*, 1978, **34**, 666.
20 D. H. Farrar, B. F. G. Johnson, J. Lewis, P. R. Raithby, and M. J. Rosales, *J. Chem. Soc., Dalton Trans.*, 1982, 2051.
21 C. R. Eady, B. F. G. Johnson, and J. Lewis, *J. Chem. Soc., Chem. Commun.*, 1976, 302.
22 W. N. Lipscomb, *Science*, 1966, **153**, 373.
23 C. R. Eady, B. F. G. Johnson, and J. Lewis, *J. Chem. Soc., Dalton Trans.*, 1975, 2606.
24 J. L. Spencer, *Inorg. Synth.*, 1979, **19**, 213.
25 SDP-Plus system, 1981, B. A. Frenz and Associates Inc., College Station, Texas and Enraf-Nonius, Delft, Holland.
26 'International Tables for *X*-Ray Crystallography,' Kynoch Press, Birmingham, 1969, vol. 4.
27 C. K. Johnson, ORTEP, Report ORNL-3794, Oak Ridge National Laboratory, Oak Ridge, Tennessee, 1965.

Received 27th August 1985; *Paper* 5/1469